Near-wall conductivity effect under a space–charge-saturated sheath in the Hall thruster*

Zhang Feng-Kui(张凤奎)[a)†], Ding Yong-Jie(丁永杰)[b)‡], Qing Shao-Wei(卿绍伟)[b)], and Wu Xian-De(吴限德)[a)]

[a)] *College of Aerospace and Civil Engineering, Harbin Engineering University, Harbin* 150001, *China*
[b)] *HIT Plasma Propulsion Laboratory, Harbin Institute of Technology, Harbin* 150001, *China*

(Received 19 September 2011; revised manuscript received 12 October 2011)

In this paper, we adopt the modified Morozov secondary electron emission model to investigate the influence of the characteristic of a space–charge-saturated sheath near the insulated wall of the Hall thruster on the near-wall conductivity, by the method of two-dimensional (2D) particle simulation (2D+3V). The results show that due to the sharp increase of collision frequency between the electrons and the wall under the space–charge-saturated sheath, the near-wall transport current under this sheath is remarkably higher than that under a classical sheath, and equals the near-wall transport current under a spatially oscillating sheath in order of magnitude. However, the transport currents under a space–charge-saturated sheath and a spatially oscillating sheath are different in mechanism, causing different current density distributions under the above two sheaths, and a great influence of channel width on the near-wall transport current under a space–charge-saturated sheath.

Keywords: saturated sheath, conductivity, current

PACS: 52.40.Kh, 94.30.cj **DOI:** 10.1088/1674-1056/20/12/125201

A Hall thruster is a kind of plasma discharging equipment in the configuration of crossed electric and magnetic fields. The transport current formed by electrons crossing the magnetic field is of crucial importance for the performance of Hall thruster. Currently, there are three main explanations for the conduction behaviour of electrons crossing the magnetic field, these being classical conductivity, Bohm-type conductivity and near-wall conductivity. In the Hall thruster, neoclassical conductivity produced by the collision between electrons and wall is far lower than experimental results; that is to say, there are abnormal conduction behaviours[1] for electrons crossing the magnetic field. Some scholars believe that the abnormal conduction behaviours inside the Hall thruster are caused by the collective oscillations of plasma, i.e. Bohm-type conductivity. In the plasma discharging equipment with a high degree of ionization, Bohm-type conductivity can be used to explain why the transport current is larger than the current produced by the collision between electrons and atoms.[2] The electron current produced by Bohm-type conductivity is inversely proportional to magnetic field intensity. The experimental results show that the magnetic field intensity in the Hall thruster increases from inside of the channel to the exit of the channel, so Bohm-type conductivity will be restrained.[3] Hence, Morozov[4] and Morozov and Savelyev[5] suggested that the electrons move to the anode after their collisions with an isolated wall, thus leading to near-wall conductivity. In the investigation of near-wall conductivity in the Hall thruster, Morozov found that the near-wall transport current gained under the assumption of a zero-thickness steady sheath is a little lower, which contradicts[6] the experimental results. Through further study on this question, Morozov and Savelyev[7,8] found that the sheath is oscillatory in the time domain with the increase of electron temperature. The research on Hall thrusters in China started late. However, there is still ongoing research on the characteristics of various sheaths[9−20] and plasma with two-dimensional (2D) PIC.[21,22] In our research, by the

*Project supported by the Fundamental Research Funds for the Central Universities (Grant No. HEUCF100212) and the National Natural Science Foundation of China (Grant Nos. 51007013, 10875024, and 10975026).

†Corresponding author. E-mail: fengkuizhang@163.com
‡Corresponding author. E-mail: dingyongjie@hit.edu.cn

© 2011 Chinese Physical Society and IOP Publishing Ltd

method of 2D particle simulation it can be shown that the sheath is periodically oscillatory[23] in the space when the electron temperature is higher. The oscillation of the sheath in the time domain may cause slow electrons to hit the wall and participate in near-wall conductivity, while the oscillation of the sheath in the space will cause slow electrons to be reflected and join in the near-wall conductivity.[24] With the increase of electron temperature, the secondary electron emission (SEE) coefficient increases, while the potential drop of the sheath decreases. When the SEE coefficient is greater than some threshold, the space–charge-saturated sheath[25] will form. Under this sheath, the collision frequency between electrons and the wall will increase sharply[26] which will have a great influence on near-wall conductivity. In this paper, we adopt the method of 2D particle simulation (2D+3V) to investigate the influence of a space–charge-saturated sheath on near-wall conductivity.

The calculating region is shown in Fig. 1. The length l_1 of the sheath region is $10\lambda_{\rm D}$. The motion area of secondary electrons starting from the wall is defined as the reflective region with a width (l_3) of $100\lambda_{\rm D}$ and the value of length (l_2) being $200\lambda_{\rm D}$ or $300\lambda_{\rm D}$ or the width of the whole channel. The value of l_2 is taken to be $200\lambda_{\rm D}$ under a spatially oscillating sheath, and $300\lambda_{\rm D}$ under a temporarily oscillating sheath and classical sheath, which can make the length l_2 of the reflective region reach half the width of the channel under the spatially oscillating sheath, temporarily oscillating sheath, and classical sheath. However, the value of l_2 is taken to be the width of the whole channel under the space–charge-saturated sheath. The grids of calculating region are divided evenly in the space. The simulated space interval should satisfy $\Delta z = \Delta r = 0.5\lambda_{\rm D}$, and the time interval should satisfy $\Delta t = 0.1\omega_{\rm ep}^{-1}$. Here, $\lambda_{\rm D}$ is the Debye length, while $\omega_{\rm ep}$ is the electron plasma frequency.

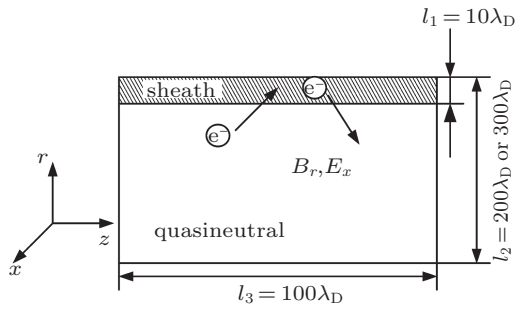


Fig. 1. Calculating region where the x direction is the axial direction; the r direction the radial direction and the z direction the azimuthal direction. B_r and E_x are added to the whole calculating region.

The electrons starting from the quasi-neutrality region (electron density $n_{\rm e} = 5 \times 10^{17}/{\rm m}^3$–$10^{18}/{\rm m}^3$) obey Maxwell distribution at a temperature of $T_{\rm e}$. When the electrons hit the wall through the sheath region, some of them are reflected[27,28] while some are absorbed by the wall, and others can knocking out secondary electrons. The lower the energy of incident electrons, the more electrons are reflected after emission. There are a great many electrons with low energy in the Hall thruster, as a result, in this paper we adopt the improved Morozov secondary electron emission model[28] to simulate the mutual effect between electrons and wall.[23] When an electron hits the wall, the following four events occur: electrons are absorbed by the wall, electrons are reflected, electrons knock out one electron, and electrons knock out two electrons. The corresponding probabilities of the four events are respectively

$$W_0(\varepsilon) = P_0 \exp\left(-\varepsilon^2/\alpha_0^2\right), \quad (1)$$

$$W_r(\varepsilon) = P_r \exp\left(-\varepsilon^2/\alpha_r^2\right), \quad (2)$$

$$W_1(\varepsilon) = 1 - W_0(\varepsilon) - W_r(\varepsilon) - W_2(\varepsilon), \quad (3)$$

$$W_2(\varepsilon) = 1 - \exp\left(-\varepsilon^2/\alpha_2^2\right), \quad (4)$$

where ε is the energy of incident electron. The corresponding parameters used in our numerical computation are set as follows: $P_0 = 0.5$, $\alpha_0 = 43.5$, $P_r = 0.5$, $\alpha_r = 30$, and $\alpha_2 = 127.9$. As shown in Fig. 2, one can find that the values from the improved SEE model are in better accordance with the experimental data of BN material[29] than those from the Morozov model. Furthermore, it is assumed that the emission of secondary electrons is Maxwellized and spatially uniform, and the average emission temperature is 1/3 times the electron temperature in the plasma bulk.[7]

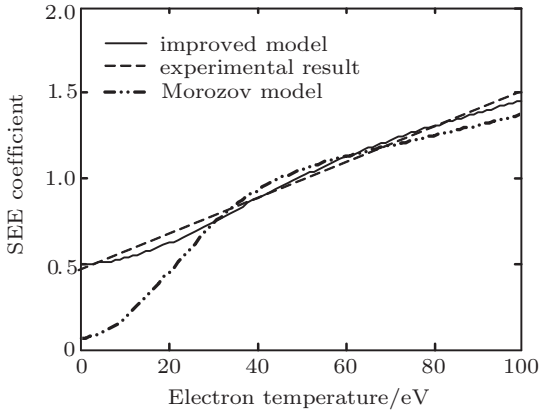


Fig. 2. Comparison of the second electron emission coefficient between the Morozov model, improved model, and experiment data.

According to the experimentally measured results of the Hall thruster, the range of electron temperatures in the channel is $T_{\rm e} < 50$ eV approximately.[30]

In this paper, the near-wall conductivity in the channel is simulated under four sheaths: the space–charge-saturated sheath, the spatially oscillating sheath, the temporarily oscillating sheath, and the classical sheath. Their corresponding electron temperatures are respectively 40, 27, 18, and 9 eV. Secondary electrons starting from the wall and slow electrons reflected by the sheath (under the spatially oscillating sheath) move according to the Boris method under a magnetic field B_r and electric field (E_x, E_r, E_z) (E_r, E_z—electric field components produced by a self-consistent sheath). The periodic boundary condition will be used for the left and the right sides of the simulated region. Following the location and the speed of electrons starting from the wall in the reflective region, the radial distribution of electron current density can be obtained by statistical average.

Radial distributions of near-wall transport current densities under a space–charge-saturated sheath, spatially oscillating sheath, temporarily oscillating sheath, and classical sheath, as well as the comparison of experimentally measured results about near-wall transport current density[31] can be shown in Fig. 3. The electron density, the axial electric field, and the radial magnetic field are respectively $n_e = 5 \times 10^{17}/m^3$, $E_x = 2000$ V/m, and $B_r = 0.015$ T. From the figure, we can see that the densities of near-wall transport current under the space–charge-saturated sheath and spatially oscillating sheath are far greater than those under a temporarily oscillating sheath and classical sheath. However, the density distribution of the near-wall transport current varies from the space–charge-saturated sheath to the spatially oscillating sheath, which is caused mainly by different physical mechanisms of near-wall conductivity between the two sheaths. The space–charge-saturated sheath relies absolutely on secondary electrons emitted after wall-hitting to participate in near-wall conductivity. The density of the near-wall transport current under a space–charge-saturated sheath converges more slowly than that under a spatially oscillating sheath because the number of secondary electrons emitted from the wall is greater, and the temperature of emission electrons is higher under the space–charge-saturated sheath. On the other hand, the spatially oscillating sheath depends mainly on slow electrons reflected by the sheath to join the near-wall conductivity. Compared with secondary electrons emitted from the wall under space–charge-saturated sheath, the slow electrons are fewer at lower temperature. Thus, its near-wall transport current density converges more quickly in the radial direction. However, the density of near-wall transport current under a spatially oscillating sheath converges more slowly than that under a temporarily oscillating sheath and a classical sheath.

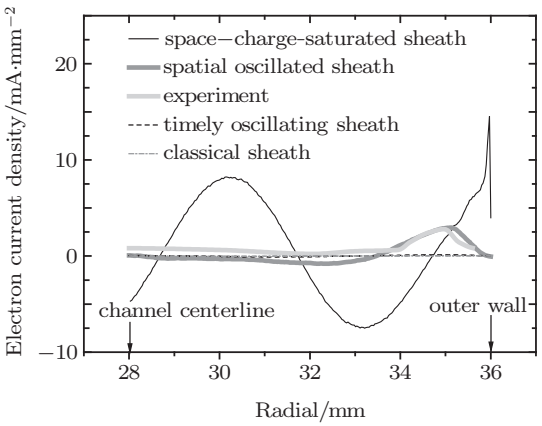


Fig. 3. Radial distributions of near-wall transport current density under a space–charge-saturated sheath, spatially oscillating sheath, temporarily oscillating sheath, and classical sheath, as well as the comparison of experimental measuring results.

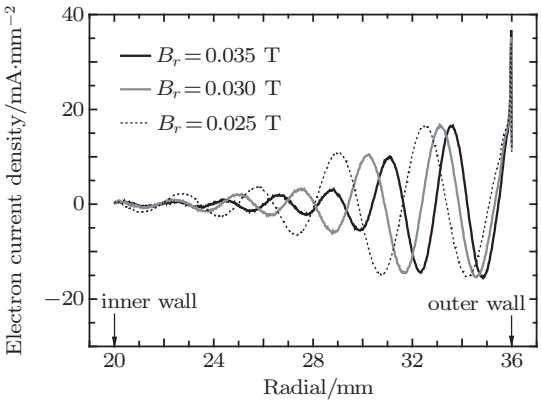


Fig. 4. Radial distributions of near-wall transport current density under a space–charge-saturated sheath and different radial magnetic fields.

Figure 4 shows radial distributions of near-wall transport current density under a space–charge-saturated sheath and different radial magnetic fields, in which the electron density and axial electric field are respectively $n_e = 10^{18}/m^3$ and $E_x = 10000$ V/m. We can find that the smaller the radial magnetic field, the more slowly the electron current density converges. The electron current density on the internal wall does not converge at 0 even when the radial magnetic field $B_r = 0.025$ T. Under the same working condition and other sheaths, the electron current density converges at 0 before arriving at the channel centre from the external wall. From the above analyses, it can be

shown that the channel width of the Hall thruster has a great influence on the near-wall conductivity under the space–charge-saturated sheath, which needs further deep research.

Figure 5 shows the intensity variations of the near-wall transport current and classical transport current with axial electric field under each sheath, in which the electron density and radial magnetic field are respectively $n_{\rm e} = 10^{18}/{\rm m}^3$ and $B_r = 0.03$ T. The electron current intensity under the corresponding sheath is obtained by the integration of the near-wall transport current density under each sheath. The intensity of the classical transport current can be calculated by the following equation:

$$I_{\rm e} = \left(\frac{\upsilon_{\rm ne}}{\upsilon_{\rm ne}^2 + \omega_{\rm ce}^2}\right) \frac{n_{\rm e} e^2}{m_{\rm e}} E_x \pi \left(r_2^2 - r_1^2\right), \qquad (5)$$

where $\upsilon_{\rm ne}$ is the collision frequency between electrons and neutral atoms, $\omega_{\rm ce}$ is the cyclotron frequency of electrons,[1] r_1 and r_2 are the radii of internal and external walls in the channel. An ATON-type Hall thruster is adopted in the calculation. The near-wall transport current density varies greatly from space–charge-saturated sheath to spatially oscillating sheath; however, their electron current intensities are more or less the same. In Fig. 5, although the near-wall transport current intensity under the space–charge-saturated sheath is larger than that under a spatially oscillating sheath, they are still of the same order of magnitude, and are far greater than the intensity of classical transport current. It can be shown that the near-wall transport current under the space–charge-saturated sheath takes up a great percentage in the Hall thruster, thus we should take into account the near-wall transport current under space–charge-saturated sheath in the Hall thruster.

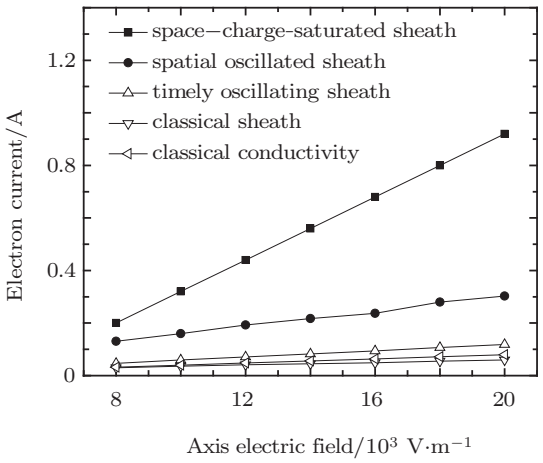


Fig. 5. Intensity variations of classical transport current and near-wall transport current with axial electric field under a space–charge-saturated sheath, spatially oscillating sheath, temporarily oscillating sheath and classical sheath.

Figure 6 shows the intensity variations of near-wall transport current and classical transport current with radial magnetic field under each sheath, in which the electron density and the axial electric field are respectively $n_{\rm e} = 10^{18}/{\rm m}^3$ and $E_x = 10^4$ V/m. From the figure, we can find that the intensities of near-wall transport current are inversely proportional to the square of the radial magnetic field ($I_{\rm e} \propto 1/B_r^2$) approximately under the oscillating sheath and classical sheath, but this is not the case for the near-wall transport current intensity under the space–charge-saturated sheath. The reason is that the convergence intervals of near-wall transport current density under the oscillating sheath and classical sheath are shorter, and the current density has already converged at 0 before arriving at the channel centre from the wall (Fig. 1), while the convergence interval of near-wall transport current density under the space–charge-saturated sheath is longer, and the near-wall transport current density has not converged at 0 after arriving at the other side of the wall from one side (Fig. 4). Therefore, the intensity of near-wall transport current under a space–charge-saturated sheath is not inversely proportional to the square of the radial magnetic field in the strict sense (Fig. 6). Moreover, the channel width has a very great influence on the near-wall conductivity under space–charge-saturated sheath, which is far

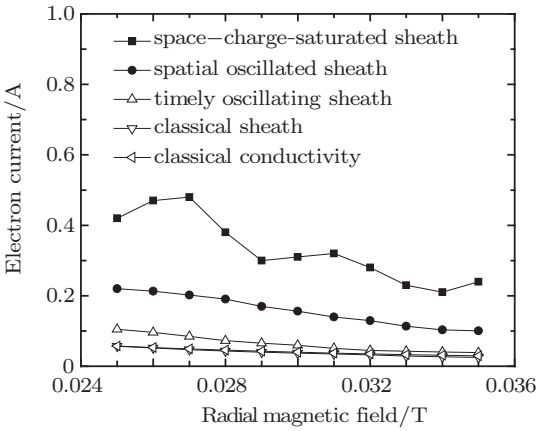


Fig. 6. Intensity variations of classical transport current and near-wall transport current with radial magnetic field under a space–charge-saturated sheath, spatially oscillating sheath, temporarily oscillating sheath, and classical sheath.

greater than its influence on the near-wall conductivities under other sheaths.

Different near-wall conductivity mechanisms under a space–charge-saturated sheath and spatially oscillating sheath may lead their near-wall transport current density distributions to be greatly different. However, their near-wall transport current intensities are more or less the same, which are of the same order of magnitude, and both are far greater than the near-wall transport currents under other sheaths and the classical transport current. The number and temperature of secondary electrons emitted from the wall under space–charge-saturated sheath may cause a longer attenuation interval of near-wall transport current density. As a result, the channel width has a great influence on the near-wall transport current under a space–charge-saturated sheath, which is far greater than its influence on the near-wall transport currents under other sheaths.

References

[1] Meezan N B and Cappelli M A 2002 *Phys. Rev.* E **66** 036401

[2] Bohm D 1949 *The Characterister of Electrical Discharge in Magnetic Field* (New York: McGraw-Hill) p. 77

[3] Morozov A I and Savelyev V V 2001 *Reviews of Plasma Physics* (New York: Consultants Bureau) p. 211

[4] Morozov A I 1968 *Prikl. Mekh. Tekh. Fuz.* **3** 19 (in Russian)

[5] Morozov A I and Savelyev V V 2001 *Plasma Phys. Rep.* **7** 570

[6] Morozov A I and Savelyev V V 2001 *Reviews of Plasma Physics* (New York: Consultants Bureau) p. 291

[7] Morozov A I and Savelyev V V 2002 *Plasma Phys. Rep.* **28** 1017

[8] Morozov A I and Savelyev V V 2004 *Plasma Phys. Rep.* **30** 299

[9] Zou X 2006 *Acta Phys. Sin.* **55** 1907 (in Chinese)

[10] Zou X, Liu H P and Gu X E 2008 *Acta Phys. Sin.* **57** 5111 (in Chinese)

[11] Zou X, Gi T K and Zou B Y 2010 *Acta Phys. Sin.* **59** 1902 (in Chinese)

[12] Wang D Y, Ma J X, Li Y R and Zhang W G 2009 *Acta Phys. Sin.* **58** 8432 (in Chinese)

[13] Li Y R, Ma J X, Zheng Y B and Zhang W G 2010 *Chin. Phys.* B **19** 085201

[14] Tan Z X, Huang Y S, Lan X F, Lu J X, Duan X J, Wang L J, Yang D W, Guo S L and Wang N Y 2010 *Chin. Phys.* B **19** 055201

[15] Da Z L, Wang Y N and Ma T C 2001 *Acta Phys. Sin.* **50** 2398 (in Chinese)

[16] Liu C S and Wang D Z 2003 *Acta Phys. Sin.* **52** 109 (in Chinese)

[17] Hou L J and Wang Y N 2003 *Acta Phys. Sin.* **52** 434 (in Chinese)

[18] Wang Z X, Liu J Y, Zou X, Liu Y and Wang X G 2004 *Acta Phys. Sin.* **53** 793 (in Chinese)

[19] Zou X, Liu J Y, Wang Z X, Gong Y, Liu Y and Wang X G 2004 *Acta Phys. Sin.* **53** 3409 (in Chinese)

[20] Duan P, Liu J Y, Gong Y, Zhang Y, Liu Y and Wang X G 2007 *Acta Phys. Sin.* **56** 7090 (in Chinese)

[21] Liu C S, Wang D Z, Liu T W and Wang Y H 2008 *Acta Phys. Sin.* **57** 6450 (in Chinese)

[22] Liu C S, Han H Y, Peng X Q, Chang Y and Wang D Z 2010 *Chin. Phys.* B **19** 035201

[23] Zhang F K, Yu D R, Ding Y J and Li H 2011 *Appl. Phys. Lett.* **98** 111501

[24] Li H, Zhang F K, Liu H and Yu D R 2010 *Phys. Plasmas* **17** 074505

[25] Barral S, Makowski K, Peradzynski Z, Gascon N and Dudeck M 2003 *Phys. Plasmas* **10** 4137

[26] Zhang F K and Ding Y J 2011 *Acta Phys. Sin.* **60** 065203 (in Chinese)

[27] Dunaevsky A, Raitses Y and Fisch N J 2003 *Phys. Plasmas* **10** 2574

[28] Morozov A I and Savelyev V V 2001 *Reviews of Plasma Physics* (New York: Consultants Bureau) p. 241

[29] Gascon N, Dudeck M and Barral S 2003 *Phys. Plasmas* **10** 4123

[30] Raitses Y, Staack D, Keidar M and Fisch N J 2005 *Phys. Plasmas* **12** 057104

[31] Bugrova A I, Morozov A I and Kharchevnikov V K 1992 *Fiz. Plazmy.* **16** 849 (in Russian)